KNOWLEDGE – International Journal
Vol. 28.2
December, 2018

PREPARATION OF CHITOSAN- SULFATHIAZOLE FILMS WITH POTENTIAL BIOMEDICAL APPLICATIONS

Dilyana Zvezdova
Prof. Assen Zlatarov University,Department of Preclinical and Clinical Subjects, zvezdova@abv.bg
Snezhina Georgieva
Prof. Assen Zlatarov University, Department of Health Care, snezhinageorgieva@abv.bg

Abstract: A series of novel chitosan-zeolite-sulfathiazole nanocomposite (CSFZ) films were prepared by using solvent casting method for wound healing application. The physicochemical properties namely thickness, folding endurance, water absorption capacity, and water vapour transmission rate (WVTR) of the films were studied. Fourier transform infrared spectroscopy (FTIR) was employed to ascertain the interaction between negatively charged zeolite and positively charged chitosan. The surface morphology of the prepared composite films was also studied by scanning electron microscopy (SEM). Due to strong hydrophilic nature of zeolite, it great lyenhances the water absorption capacities of the prepared nanocomposite films. In addition, the presence of zeolite in the said films also increases the mechanical strength. The above analysis suggested that the CSFZ films could be used as potential candidates for wound healing application.
Keywords: Chitosan-zeolite-sulfathiazole nanocomposite, FTIR spectroscopy, Water absorption capacity, Water vapour transmission rate

1. INTRODUCTION

Chitosan is the second largest biopolymer after cellulose. Chitosan is interesting because of its low cost, availability of amino and hydroxyl groups in the structure, which are potential to react. However, the chitosan has limitation in their application due to its low surface area, and mechanic resistance. In order to overcome the limitation, several works have been conducted on the development of chitosan based materials such as films [1-3]. Chitosan is inexpensive and nontoxic and possesses reactive amino groups. It has been shown to be useful in many different areas as an antimicrobial compound in agriculture, as a potential elicitor of plant defense responses, as a flocculating agent in wastewater treatment, as an additive in the food industry, as a hydrating agent in cosmetics, and more recently as a pharmaceutical agent in biomedicine. In this context, the antimicrobial activity of chitosan and its derivatives against different groups of microorganisms, such as bacteria and fungi, has received considerable attention in recent years.

Skin is often injured by wounds or physical traumas. Damages to skin commence a series of complex and well-orchestrated events of repair processes that result in the complete reestablishment of the integrity of wounded tissue and the restoration of this functional barrier. However, the morbidity of the prolonged periods required for the repair and regeneration of the injured tissue, the bleeding, the risk of infections and septicemias, and the keloids and scar formation cause the deep lesions to the skin to remain a major clinical problem[4-6]. Although new therapeutic approaches for the treatment of such large and full thickness skin lesions have made progress, there is still need for better methods to improve wound healing and recovery especially in severely wounded patients. One of the approaches for treating the wounds and diminishing the risk of wound infection is the use of biocompatible composites incorporated with antibacterial agents. Ion-exchange zeolite has attracted a lot of attention due to its renewable nature, good biocompatibility and excellent physical properties, which are important for a range of applications in pharmaceutical and biomedical fields. Several polymers are used for the fabrication of such composites including pectin, chitin, chitosan, alginate and gelatin. Among these, chitosan is regarded to be a suitable matrix due to its natural abundance, biocompatibility, biodegradability and nonimmunogenicity [6]. Recently, inorganic minerals such as clays and zeolites have become important in comparison with the conventional antibacterial agents [8-10]. The incorporation of metallic ions whitens the silicate framework which is allowed for their controlled release and prevents the concentration dependent toxicity. In the present study, we investigated the potential of chitosan-zeolite-sulfathiazole based nanocomposite for wound healing.

2. EXPERIMENTAL PART

Materials.

Chitosan (CS) with a degree of deacetylation 79% was obtained as a gift sample from shrimp shells, Sulfathiazole (SF) from Sigma-Aldrich, and Zeolite (Z) was purchased from Kardzhali region. All chemicals were used as received without further purification.

Preparation of chitosan film.

First, 1% (w/v) chitosan solution was prepared by dissolving 1 g of chitosan in 100 mL of 1% (v/v) aqueous acetic acid under continuous magnetic stirring. Then the solution was allowed to keep at room temperature for one or two days to remove the air bubbles formed during stirring so as to obtain a clear solution. After that the clear solution was cast evenly into a petri plate and allowed to dry at 60 °C in an oven. After drying, the chitosan film was peeled off and stored in desiccator for further study.

Preparation of chitosan-sulfathiazole-zeolite films (CSFZ).

The nanocomposite films were prepared by using the above-mentioned method. In brief, 1% (w/v) CS solution, 0.25% (w/v) sulfathiazole (SF) and 0.25% (w/v) zeolite (Z) solution were prepared separately. Then CS solution was added dropwise into the mixture of T and Z solution in different ratios under continuous magnetic stirring at 52°C to obtain a solution mixture (Table 1). Finally, the solution mixture was cast into a petri plate and dried at 60 °C to evaporate the solvent for the formation of CSFZ film.

Table 1. Proportion of chitosan and sulfathiazole-zeolite in nanocomposite films.

S. No.	Sample code	Chitosan (mL)	Sulfathiazole-Zeolite (mL)
1	Cs	25	-
2	CSFZ 1	10	10
3	CSFZ 2	20	10
4	CSFZ 3	30	10
5	CSFZ 4	40	10
6	CSFZ 5	50	10

Characterization of CSFZ film

The IR spectrum of the pellets was acquired using infrared spectrometer Nicolet iS 50 FTIR in the range of 4000-400 cm -1. Approximately 1mg of the sample was well mixed into 300 mg KBr powder and then finely pulverized and put into a pellet-forming die. A force of approximately 6 tons was applied under vacuum for several minutes to form transparent pellets.

Folding endurance

The folding endurance of the CSFZ films was measured to find the flexibility needed to handle the films comfortably, safely, and carefully on the wound surface. The folding endurance was determined manually by repeatedly folding the film at the same point until it broke or folded up to 300 times. The number of times of folding without any breakage gave the exact value of folding endurance of the CSFZ film. It was performed three times for each film to obtain an average value.

Thickness and mass measurement of the CSFZ films

Thickness is a major factor that greatly affects the functional properties of wound dressing materials. The thicknesses of the CSFZ films were measured using an electronic digital micrometer (Kinex CZ) and randomly selecting four positions on each film. The mean was used to express the thickness of the films. To determine the mass uniformity of each CSFZ film, four pieces of equal sizes were cut from different positions of each CSFZ film followed by weighing their respective masses with electronic balance and eventually, these values were used to calculate the average mass.

Water absorption capacity

For water absorption capacities, the preweighed CSFZ films (25 mm x 25 mm) were individually immersed in 20 mL of freshly prepared 0.9% saline solution at room temperature. Then, the soaked films were withdrawn from the medium at pre-determined time interval. The swollen weights of the CSFZ films were determined after removing excess surface water on the films with filter paper followed by placing them back into the same saline solution. Percentage swelling of the CSFZ films was calculated according to the following equation:

$$\text{Swelling (\%)} = [W_f - W_i/W_j] \times 100 \quad (1)$$

where W_f is the weight of the wet film and W_j is the initial weight of the film.

Water vapour transmission rate

Water vapour transmission rate (WVTR) was determined gravimetrically according to the modified ASTM E96-95 standard method. Succinctly, a CSFZ film of a suitable dimension was mounted on a circular opening of a WVT cup containing 20 mL of distilled water. The WVT cup was accurately weighed and placed in an incubator at 25 $^{\circ}$C. Then the WVT cup was re-weighed periodically at 24, 48, and 72 h and then a rate of change in mass was plotted as function of time for each CSFZ film. Finally, the WVTR was calculated using the following equation:

$$WVTR(gm^{-2}\ day^{-1}) = [M \times 24/T\text{-}A] \quad (2)$$

where M represents change in weight, T is time during which the change in weight occurred, and A is the exposed area of the film (m^2).

Dressing pH

First, the CSFZ films were separately immersed in normal saline solution until it reached equilibrium. After that each CSFZ film was removed from the normal saline solution and the same solution was taken into consideration for determining the dressing pH of the said films using a digital pH meter. All tests were performed three times and the average values were recorded.

Porosity measurement

The porosity of the CSFZ films was determined using the liquid displacement method. In brief, the weight of each CSFZ film with a dimension of 1cm x 1 cm was recorded and then the film was put into a beaker containing 5 mL of absolute ethanol for 24 h or until it reached equilibrium. After that the CSFZ film was taken out and further weighed. The porosity of the CSFZ films was calculated using the following equation:

$$\text{Porosity} = [(W_2 - W_1 - W_3)/(W_2 - W_3)] \times 100 \quad (3)$$

where W_1 represents the initial known weight of a film, W_2 is the sum of the weights of ethanol and the immersed film, and W_3 is the weight of ethanol after the removal of each film.

3. RESULTS AND DISCUSSION

Characterization of CSFZ films

Fourier transform infrared spectroscopy (FTIR)

FTIR spectra of chitosan (CS), sulfathiazole (SF), zeolite (Z), and chitosan-sulfathiazole-zeolite nanocomposite (CSFZ) films are displayed in Fig. 1. The FTIR spectrum of Z shows a peak at 1065.61 cm^{-1} that belongs to Si-O-Si linkage. In addition, the characteristic absorption peaks are found at ~3628.71 cm^{-1} (stretching vibration of Al OH and Si—OH), at 3446 cm^{-1} (stretching vibration of O H and H—O—H groups), at 1636.41 cm^{-1} (H—O—H bending vibration), at 794.54 cm^{-1} (Al—Al—OH bending frequency), and at 507 cm^{-1} (bending vibration of Si—O). The spectrum of CSFZ nanocomposite film (Fig. 1) shows a characteristic band at 3431.78 cm^{-1} that is due to a hydrogen bonding formation between the functional groups of C (O—H and N—H groups) and Z (O—H groups).

In the IR spectra of sulfathiazole polymorphs, the first interesting region is 3500-3200 cm^{-1}, as it is here that any differences in H-bonding will have greatest effect. Each phase has specific bands in the NH stretching vibration region (Fig. 1). It is clear from Table 1 that the characteristic fundamental bands of form I corresponding to the N-H stretching vibrations at 3464 and 3358 cm^{-1} are shifted to lower wavenumber (3320 and 3280 cm^{-1}) in form III due to the increased intermolecular hydrogen bonding present. For form V, the peak at highest wavenumber is divided into two overlapping bands at 3443 and 3418 cm^{-1}. Each polymorph also exhibits a characteristic spectrum in the IR fingerprint region (1800-650 cm^{-1}). Generally, the bands corresponding to the $1NH_2$ vibration can be observed at 1650-1590 cm^{-1}. Polymorphs III and V have $1NH_2$ vibrations at 1628, 1594 and 1644,1596 cm^{-1}, respectively. On the other hand, polymorph I has $1NH_2$ vibrations at 1634, 1627 and 1592 cm^{-1}.The wagging NH_2 mode for the three polymorphs is observed around 730 cm^{-1}. The bands around 1323 and 1128cm^{-1} are assigned to asymmetric and symmetric stretching vibrations of SO_2. In addition, the IR spectra show a strong band around 1530 cm^{-1}, attributed to the stretching vibration of C=N of the thiazole ring.

Table 1Observed and calculated frequencies for sulfathiazole polymorphs I, III, V between 3700 and 650 cm^{-1}.

Calculated (cm^{-1})	Band assignment	Polymorph I observed (cm^{-1})
3550	ν_{as} (NH2)	3464
3442	ν_{s} (NH2)	3358
3319	ν (NH)	
3164	ν (CH)	3136
3131	ν (CH)	3116
3105	ν (CH)	3094
3073	ν (CH)	3072

3064	ν (CH)	3058
3031	ν (CH)	3014
1607	l (NH2)	1634,1627
1586	l (NH2) + Vring (phenyl)	1592
		1574
1577	ν (C = N) (thiazole)	1534
1567	ν (CC) (thiazole)	1499
1481	l (CH) (phenyl) + ν (C-NH2)	1417
1224	Vas (SO2)	1334
1174	l(CH) +1 (CNC)	1290
1159	l (CH) (phenyl)	1279
1107	l (CH) (phenyl)	1184
1011	νs(SO2)	1128
1087	ν(C-S) +1 (CH)	1086
1081	l (CH) +1 (NH) + ν (C-S)	1073
1049	l (CH)+l (NH)	1007
916	γ (CH) (phenyl)	929
816	γ (CC)	857
800	γ (CH)	829
700	δ (NH)	734
694	γ (CC) (phenyl)	684

Vibrational modes—*ν:* stretching; l: in-plane deformation; *γ*: out-of-plane deformation. Subscripts: s: symmetric; as: asymmetric

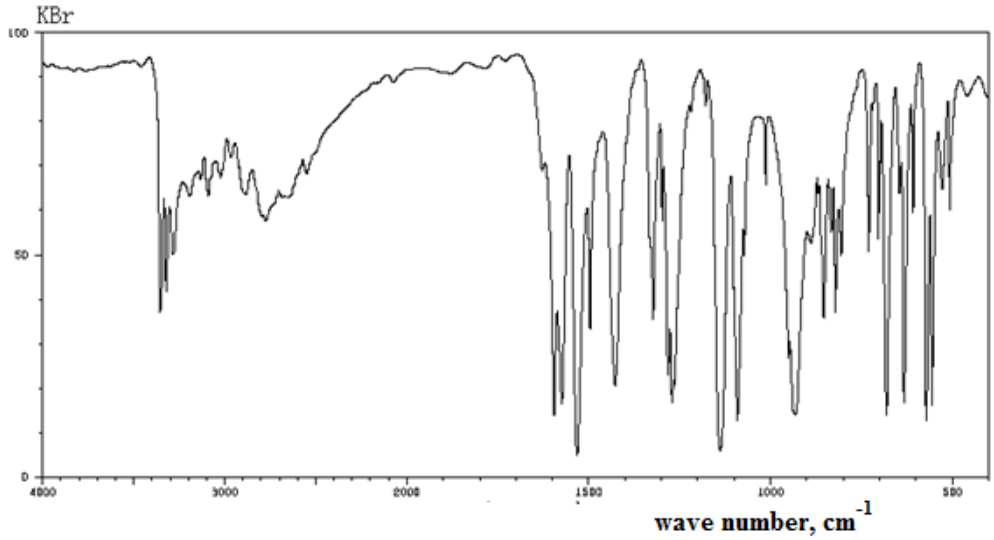

Fig.1 FTIR spectra of CSFZ film

Thickness and mass measurement of CSFZ films

The analysis of thicknesses of pure chitosan and CSFZ films with varying ratios of C and Z is portrayed in Table 2. To obtain uniform thickness throughout the nanocomposite films, petri plates with the same diameters and equal volumes of all the prepared solutions were used. The thicknesses of all CSFZ films were in the range between 17.5 ±10 |am and 36 ±19 |am. It was found out that the thicknesses of the nanocomposite films increased with increasing the chitosan content in the film forming solution that might be due to enhanced viscosity of C. The mass of 1 cm x 1 cm of the CSFZ film was calculated for each prepared film, and it was in the range between 17.00 ± 1.00 mg and 25.00 ± 2.06 mg. From the result, it was found out that there was no significant variation in the masses of the CSFZ nanocomposite films. This result indicated that the method adopted for the preparation of the CSFZ films was consistent.

Folding endurance

Each CSFZ film was individually folded repeatedly in the same place to find their folding strength and data are displayed in Table 2.

Table 2. Physical properties of CSFZ films in terms of thickness, mass, and folding endurance.

Sample code	Thickness (µm)	Mass (mg)	Folding endurance
CS	21.00	22.00	215.00
CSFZ 1	17.50	18.00	190.78
CSFZ 2	25.55	29.00	200.00
CSFZ 3	28.50	28.50	199.50
CSFZ 4	29.90	29.70	187.25
CSFZ 5	36.50	35.00	182.50

The table shows that the folding strength of the CSFZ films increases with decreasing the content of zeolite from 50% to 20% with respect to chitosan in the said films. Further reduction of the zeolite content may decrease the folding strength of the nanocomposite films. It can be seen from Table 2 that CSFZ 2 nanocomposite film (200.00) shows the highest folding strength, whereas the CSFZ 1 nanocomposite film (200) shows the lowest one among all prepared nanocomposite films. Therefore, it can be said that the presence of zeolite in the right proportion in the solution mixture greatly enhances the mechanical strength of the nanocomposite films.

Water absorption capacity

Ideally, a wound dressing material should absorb wound fluid while it is applied on the wound bed and thus, it maintains a certain level of moist environment at the wound bed. Water absorption capacity is an important factor of any wound dressing material and prevents dehydration of the tissue, inhibits microorganism growth, and also protects wound maceration. As depicted in Fig. 2, it was found out that the water absorption capacities of all CSFZ films increased over a period of time. Apart from this, it also showed that CSFZ 4 had the highest water absorption capacity among all prepared CSFZ films. It is expected that due to the hydrophilic nature and water holding capacity of zeolite, it enhances the water absorption capacity of the CSFZ 4 nanocomposite film. Furthermore, the results showed that the water absorption capacity of the prepared CSFZ films increased with increasing the content of C in the composites.

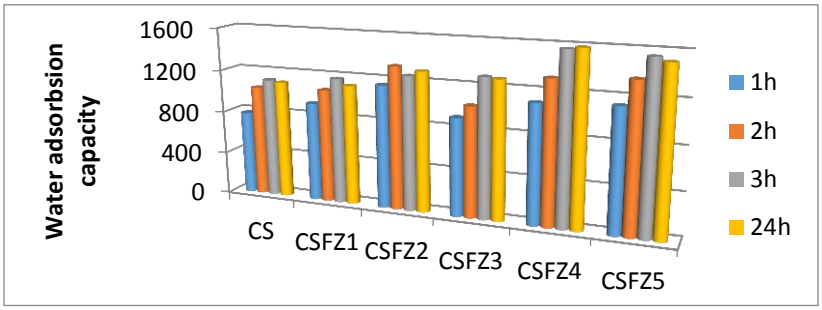

Fig. 2. Water absorption capacity of pure chitosan (CS) and CSFZ films.

Water vapour transmission rate (WVTR)

A dressing used for wound healing purposes should maintain water loss from the wound surface at an optimal rate. The high value of water vapour loss may lead to dehydration of the wound and adherence of the dressing to the wound surface, whereas the low value of water vapour loss might lead to accumulation of wound exudates that may accelerate the risk of bacterial growth and also delay the wound healing process. The WVTR values of the pure C and CSFZ films are shown in Fig. 3. The pure CS shows reasonably good WVTR, which is further increased by the addition of tertsef and zeolite. The WVTR value of the CSFZ 4 nanocomposite film is near the above-mentioned recommended range of an ideal wound dressing.

Dressing pH

Dressing pH is an important parameter for wound dressing, which facilitates not only the control of infection at the wound surface but also accelerates the formation of fibroblast proliferation. Ideally, a wound dressing should maintain a slightly acidic environment at wound surface (because the pH of normal human skin ranges between 4.0 and 6.8) and thus it would accelerate the wound healing process compared to neutral and alkaline environments. The CSFZ films show dressing pH in the range between 5.60 and 6.80, which is presented in Fig. 4. From this result, it can be concluded that the CSFZ nanocomposite film has an ability to provide an acidic environment to the wound surface, where CSFZ can enhance cell proliferation and fibroblast formation as well.

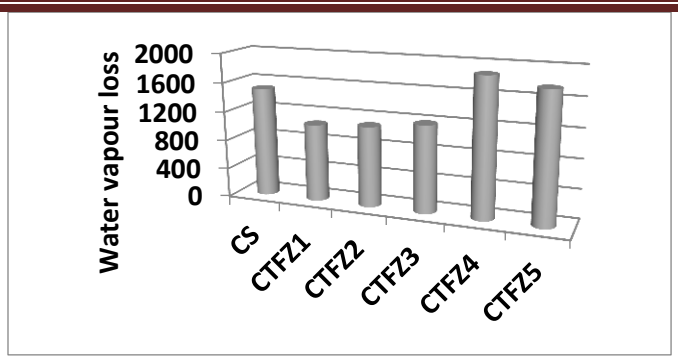

Fig. 3. Water Vapour Transmission Rate value of chitosan and CSFZ film.

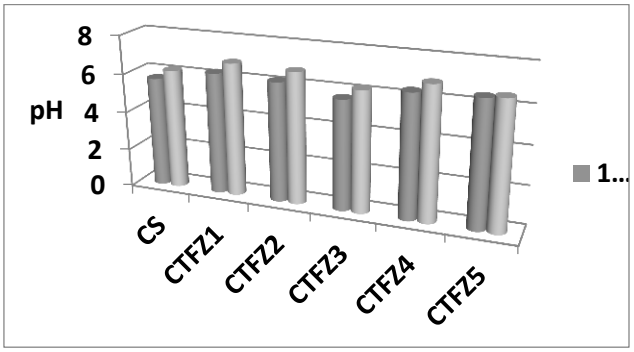

Fig. 4. Dressing pH of pure CS and CSFZ films.

Porosity measurement

The porosity of the CSFZ films was determined by the liquid displacement method using absolute ethanol and the results are shown in Fig. 5. The porosity of pure chitosan film increased from 70% to 90% significantly with the incorporation of sulfathiazole and zeolite. The porosity of the nanocomposite films affected not only their swelling abilities but also their WVTRs. The decreasing values of water absorption capacity and WVTR might be due to low porosity as shown in Fig. 3 and 4, respectively. This result confirmed that there was a direct influence of porosity on water absorption capacity and WVTR as well.

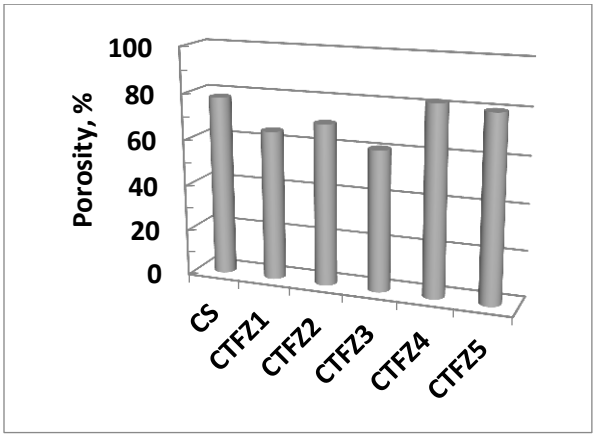

Fig. 5. Porosity evaluation of the nanocomposite films.

CONCLUSION

A series of novel chitosan-sulfathiazole-zeolite nanocomposite films were prepared for wound healing application by using the solvent casting method. The contents of chitosan, sulfathiazole and zeolite in the solution mixture were optimized on the basis of folding endurance of the prepared nanocomposite films, followed by

studying water absorption capacities, WVTRs, and porosity measurements. More interestingly, the incorporation of an appropriate amount of zeolite in the solution mixture with respect to chitosan in order to produce the nanocomposite films dramatically improved almost all properties which are required from an ideal wound dressing material. FTIR spectra confirmed the H-bonding interactions between the hydroxyl groups of zeolite with the hydroxyl and amino groups of chitosan.

REFERENCES

[1]. C. Pillai, W. Paul and C. Sharma. Prog. Polym. Sci., vol. 34, p. 641–678, 2009.
[2]. K. Murakami, H. Aoki, S. Nakamura, S. I. Nakamura, M. Takikawa, M. Hanzawa, S. Kishimoto, H. Hattori, Y. Tanaka, T. Kiyosawa, Y. Sato and M. Ishihara. Biomaterials, 31, p. 83–90, 2010.
[3]. Boucard N., C. Viton, D. Agay, E. Mari, T. Roger, Y. Chancerelle and A. Domard. Biomaterials, vol. 28, p. 3478–3488, 2007.
[4]. Patrulea V., V. Ostafe, G. Borchard and O. Jordan. Eur. J. Pharm. Biopharm., vol. 97, p. 417–426, 2015.
[5]. Usman A., K. M. Zia, M. Zuber, S. Tabasum, S. Rehman and F. Zia. Int. J. Biol. Macromol., vol. 86, p. 630–645, 2016.
[6]. Jayakumar R., M. Prabaharan, P.T. Sudheesh Kumar, S.V. Nair and H. Tamura. Biotechnol. Adv., vol. 29, p. 322–337, 2011.
[7]. Bano I., M. Arshad, T. Yasin, M.A. Ghauri and M. Younus. Int. J. Biol. Macromol., vol. 102, p. 380–383, 2017.
[8]. Chen H., X. Xing, H. Tan, Y. Jia, T. Zhou, Y. Chen, Z. Ling and X. Hu. Mater. Sci. Eng. C, vol. 70, p. 287–295, 2017.
[9]. Arifin D.Y., L.Y. Lee and C.H. Wang. Adv.Drug Deliv. Rev., vol. 58, p. 1274–1325, 2006.
[10]. Lin C.C. and A.T. Metters. Adv. Drug Deliv. Rev., vol. 58, p. 1379–1408, 2006.